Engineering Design-II

BME 350

Doppler Radar based unobtrusive respiration monitoring system

Advisor:

Dr. Taufiq Hasan, Assistant Professor,BME,BUET

Team Members:

Sushanto Kumar Saha

Student Id- 1518003

Mir Maheen Labib Al Haque

Student Id- 1518021

Date of submission- 23/07/2018

Abstract:

Respiratory rate (RR), or the number of breaths per minute, is a vital clinical sign that can actually provide insight into one's **general state of health** and can also be a **valuable indicator** of underlying medical conditions of individuals. Among several methods, non-contact characteristics of Doppler Radar sensor provides an unobtrusive means of continuous respiration detection and monitoring. No attachment of physical sensor or special clothing and preparation is needed for this system which makes this system easily applicable for both home and hospital usage. In this project, it is aimed to implement a sustainable Doppler Radar based respiration monitoring system and analyze the accuracy of respiration monitoring system with present established systems. In this regard, a respiration monitoring circuit is developed and further processing was done to to examine their appropriateness as well as sustainability of the respiration monitoring system. Results show that the respiration monitoring rates successfully meet the needs to have a non-contact unobtrusive respiration monitoring system. It is expected that the present methodology and analysis procedure will provide a great insight for future optimization of respiration monitoring systems.

TABLE OF CONTENTS

LIST OF FIGURES..... 4-5

BODY OF THE REPORT..... 6-

i. INTRODUCTION..... 6-8

ii. BACKGROUND..... 9-23

iii. PRELIMINARY DESIGN..... 23-27

iv. FABRICATION PROCESS..... 28-33

v. FINAL PROTOTYPE.....33-35

vi. DATA COLLECTION AND TESTING.....35-38

RESULTS.....39-45

DISCUSSION.....46-47

CONCLUSION.....48-49

REFERENCES.....50-51

APPENDIX.....52-54

i. List of acronyms.....52

ii. User Defined Code.....53-54

List of Figures:

Fig. 1.1: The prevalence of respiratory diseases worldwide signifies the importance of respiratory monitoring systems ……..6

Fig. 1.2: Fig. 1.2: Chest electrode based respiration monitoring system……7

Fig. 1.3: Spirometry based respiration monitoring system……

Fig. 1.4: Respiration Monitor Belt……

Fig 2.1: Figure 2.1: Detection theory of heartbeat and breathing using continuous wave Doppler radar.
……9

Fig 3.1: Proteus Design of Circuit A……..24

Fig 3.2: Proteus Design of Circuit B……25

Fig 3.3: Proteus Design of circuit C……..26

Fig 4.1: Proteus design of final amplifier circuit…… 13

Figure 5.1: CDM 324 and HB 100 Doppler Radar sensors from left to right……

Figure 5.2: Amplifier Module INA 118P and circuit diagram……34

Fig 5.3.1: Blutooth HC-05……34

Fig 5.3.2: Arduino Uno……35

Fig 5.3.3: Arduino Nano……35

Fig 5.3.4: LiPo Battery……

Fig 6.1: Final Circuit Design for Hardwa……36

Fig 7.1: Raw Data……40

Fig 7.2: Power Density Spectrum using fft……41

Fig 7.3: Filtered Data……41

Fig 7.4: Smoothed Data……42

Fig 7.4: Final Data……43
.

INTRODUCTION

The respiratory rate is one of the four vital signs which is a core component of regular health monitoring. Normal respiration rate of humans can vary according to age, gender, physical exercise, different medical conditions etc. In normal, 12-18 breaths per minutes represent a sound respiration rate for an adult. Slowing down of respiratory rate (bradypnea or apnea) or increasing of respiratory rate (tachypnea) can be a warning of clinical deterioration or impending respiratory arrest. Besides in sleep monitoring system, sophisticated respiratory rate and pattern monitoring are required during polysomnography. Respiratory monitors are also used in homes for infant studies.

Respiratory diseases impose an immense worldwide health burden. According to the forum of International Respiratory Societies - .

• An estimated 65 million people have moderate to severe chronic obstructive pulmonary disease (COPD), from which about 3 million die each year. [2, 3].

• About 334 million people suffer from asthma [4], which is the most common chronic disease of childhood, affecting 14% of children globally.

• For decades, acute lower respiratory tract infections have been among the top three causes of death and disability among both children and adults

• In 2015, 10.4 million people developed tuberculosis (TB) and 1.4 million people died from it.

.• More than 100 million people suffer from sleep-disordered breathing [2].

It can be easily understood from the statistical values that respiratory diseases has become a great concern worldwide. And the very first symptom of respiratory diseases can be identified with observing breathing rate and patterns. So, the importance of respiratory monitoring system is beyond explanation.

Fig. 1.1: The prevalence of respiratory diseases worldwide signifies the importance of respiratory monitoring systems

There are several respiratory monitoring systems which are present in common market and used by hospitals.

1. Electrode and wired based respiratory monitors: This system uses chest electrodes to measure heart rate. Normally, it is an multipurpose system which combines heart rate, pulse and some other features as well. This product is available worldwide from several companies like General Electric, PHILIPS, OMCRON, Hisense etc.

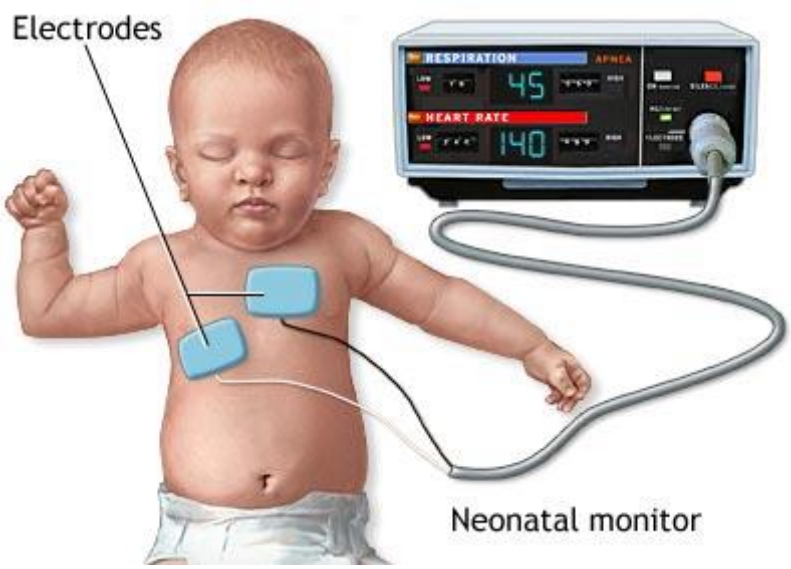

Fig. 1.2: Chest electrode based respiration monitoring system

2. Spirometer based respiration monitoring system: **Spirometry** (meaning *the measuring of breath*) is the most common of the pulmonary function tests (PFTs). Spirometry is helpful in assessing breathing patterns that identify conditions such as asthma, pulmonary fibrosis, cystic fibrosis, and COPD. It is also helpful as part of a system of health surveillance, in which breathing patterns are measured over time. Biopac, Schillers, Sparo labs are renowned manufacturers of spirometers.

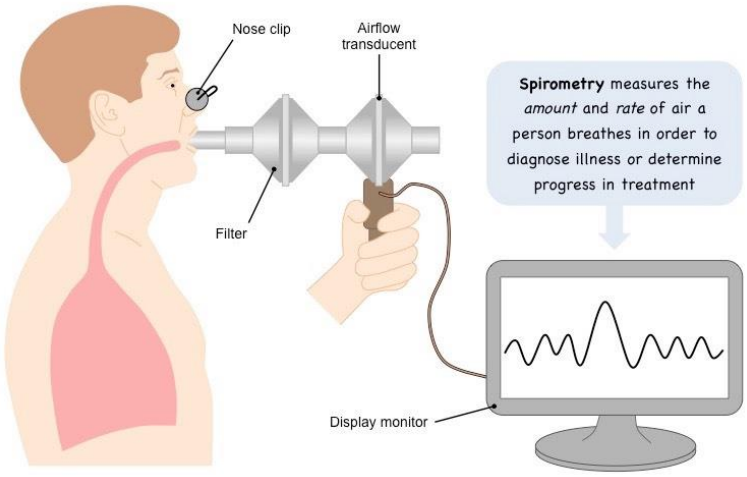

Fig. 1.3: Spirometry based respiration monitoring system

3. Respiration Monitoring Belt: The Respiration Monitor Belt is used with the Gas Pressure Sensor to measure human respiration. Vernier, Neulog etc. manufacturer companies are renowned for their respiration monitor belts.

Fig. 1.3: Respiration Monitor Belt

All of the products that are available in the market are trustworthy and serves good purposes. Still they have some drawbacks considering some special cases.

- Wired and electrode based respiration monitor systems are not suitable for infants, burnt patients and neonates. It also makes the environment clumsy. It is not suitable for usage at home.
- Old and aged patients and patient with lung and heart problem finds it difficult when breathing using spirometry. It is not suitable for continuous monitoring because it needs body contact and spirometer to breath.

- Respiration monitor belts need forced breathing. It's not suitable for continuous breathing monitoring.

The motivation of this project is to address these limitations by developing a Doppler Radar Based unobtrusive continuous respiration monitoring system for both home and hospital usage and making it user friendly, portable and cost effective.

Background

Fundamentals of Doppler Radar

The concept of contactless vital signal monitoring using microwave signals has been explored since the 1970s [32]. Since then a lot of research has been done to improve the performance of the system both in analog circuit design of high frequency carrier signal as well as signal processing of base-banded signal. Different choices of radio frequencies have been explored starting from 1150 MHz to detect vitals through earthquake rubble and concrete [16] all the way up to Ka band [39] to improve detection sensitivity. Different receiver architectures [31] and techniques to compensate for phase noise [29] have been proposed and tested. Over the years, RADAR modules have been reduced from bulky military grade systems mounted on a tripod to a relatively small BiCMOS chips suitable for integration in portable electronic devices [20]. A comprehensive study on RADAR technology for vital signal detection can be found in [27].

Building on top of this massive prior knowledge, Hb 100 sensor allows the feasibility of contactless vital sensing using RADAR. 24 GHz direct conversion quadrature RADAR module was selected.

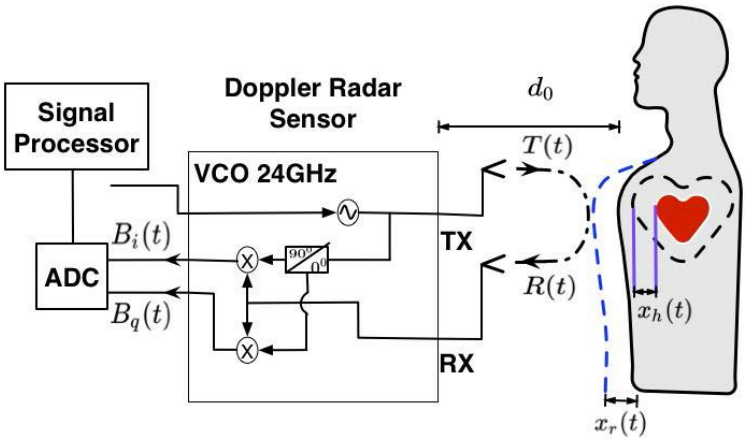

Figure 2.1: Detection theory of heartbeat and breathing using continuous wave Doppler radar. The fundamental principle behind detecting vital signals using continuous wave Doppler radar is demonstrated in figure 2.

The module transmits a single tone T(t) on a carrier frequency of f, wavelength of $\Phi(t) = c/f$, combined with phase noise $\Phi(t)$ from the oscillator, given by the equation (1):

$$T(t) = \cos(2\pi ft + \phi(t))$$

Assume that T(t) traverses a distance of d0 and hits a human's body generating periodic chest movements due to respiration and heart beating. If the displacement of chest due to respiration is $x_r(t)$ and the displacement of heart due to heart beat is $x_h(t)$, the overall movement can be expressed as $x(t) = x_r(t) + x_h(t)$. As a result, the reflected signal R(t).received by the radar is given by:

$$R(t) \approx A_r \cos(2\pi ft - \frac{4\pi d_0}{\lambda} - \frac{4\pi x(t)}{\lambda} + \phi(t - \frac{2d_0}{c})) \quad (2)$$

R(t) is a time delayed and amplitude reduced version (reduced to A_r) of the transmitted signal T(t). Most importantly, the information of x(t) is phase modulated in R(t) in addition to the distance between the human body and the radar, d_0 and a time delayed version of the phase noise $\phi(t - \frac{2d_0}{c})$. After R(t) goes through a Low Noise Amplifier

(LNA), it is converted to baseband by a mixer that multiplies the received signal with a copy of the transmitted signal. The output of the mixer gives the difference or intermediate frequencies (IF). The receiver thus gets rid off any information related to carrier frequency (2πft) and preserves the change in phase of the signal corresponding to x(t) which we want to capture. In this study we use a quadrature receiver, which compensates for null detection points a problem faced by single channel receivers [19]. In a quadrature receiver, R(t) is split into two components and multiplied by two copies of transmitted signal that are 90o out of phase with each other. The output is thus a pair of orthonormal baseband signals, $B_i(t)$ and $B_q(t)$, expressed by equation 3.

$$B_i(t) = \cos(\theta + \frac{\pi}{4} + \frac{4\pi x(t)}{\lambda} + \Delta\phi(t))$$
$$B_q(t) = \cos(\theta - \frac{\pi}{4} + \frac{4\pi x(t)}{\lambda} + \Delta\phi(t)) \quad (3)$$

Here, $\theta = 4\pi d_0/\lambda + \theta_0$, contains the target distance information d_0. and ΔΦ(t) is the residual oscillator phase noise. The portion of interest is therefore the phase modulation due to physical and physiological movements x(t) given by $\frac{4\pi x(t)}{\lambda}$.

Since $B_i(t)$ and $B_q(t)$ have a 90 degree phase difference, the quadrature receiver ensures that at least one of the baseband channels is not at a null detection point [19]. For example, if the distance d_0 that makes up _ is such that ɵ is ɵ=π/4, then $B_i(t)$ and $B_q(t)$ can be approximated as

$$B_i(t) \approx \frac{4\pi x(t)}{\lambda} + \Delta\phi(t)$$
$$B_q(t) \approx 1 - [\frac{4\pi x(t)}{\lambda} + \Delta\phi(t)]^2 \quad (4)$$

Here Bi(t) is at an optimal point with full sensitivity, while Bq(t) is at a null point with least sensitivity. Thus phase information can be recovered from one channel even if the other is at a null point. The next step is to process the two channels to get a output signal that is compensated for null-point. There are various null-point compensation

techniques including frequency tuning technique [38], complex signal demodulation [28] and arctangent demodulation [34]. In this study we used a simpler technique of selecting one optimal channel that is farthest from the null point using to heart beat is xh(t), the overall movement can be expressed interquartile range. Higher interquartile range of a channel will indicate that it is further away from the null-point, thus the optimal channel. The output signal is referred to 'Intermediate' frequency (IF).

Preliminary Design:

In this project, at first the output signal of the HB100 Doppler radar sensor was tested using the oscilloscope to understand the signal properties. The signal was within 0.8 mV range. For signal acquisition and processing we used Arduino microcontroller. But the ADC quantization level was about 1mV. So we had to use an analog amplifier circuit. Then several circuits were designed to get the best acquisition of respiration data and further used for analysis. The designs are referred as Circuit A, Circuit B and Circuit C.

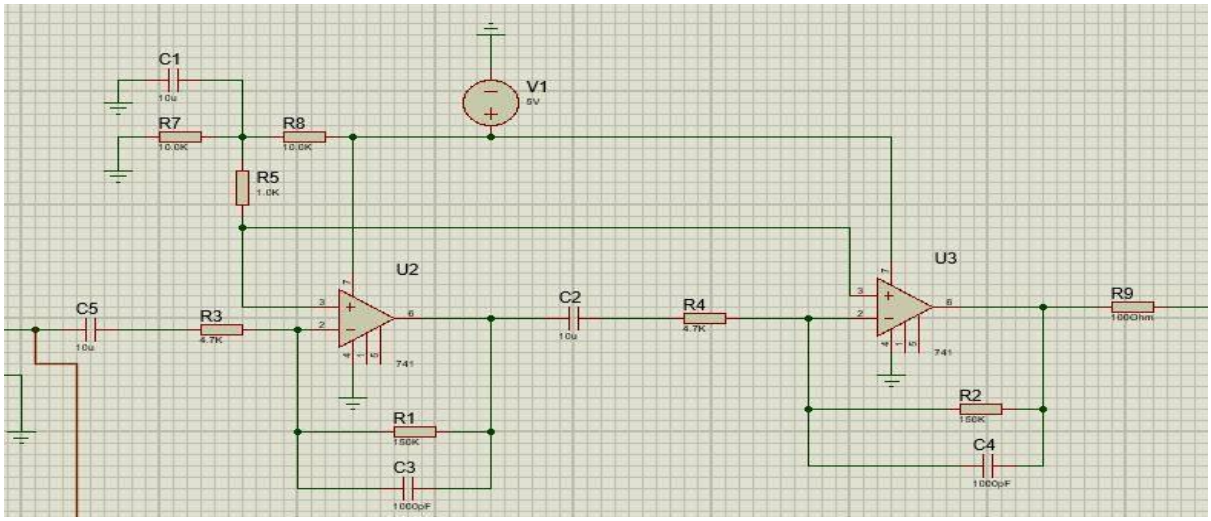

Fig 3.1: Proteus Design of Circuit A

In this first circuit A, LM 741 operation amplifier circuit was used to amplify the acquired signal. The circuit was powered up by signal generator available in the instrumentation laboratory. The received signal was analyzed in the oscilloscope. It was found that there were a lot of noises present in the received amplified signal which was not good enough for further processing.

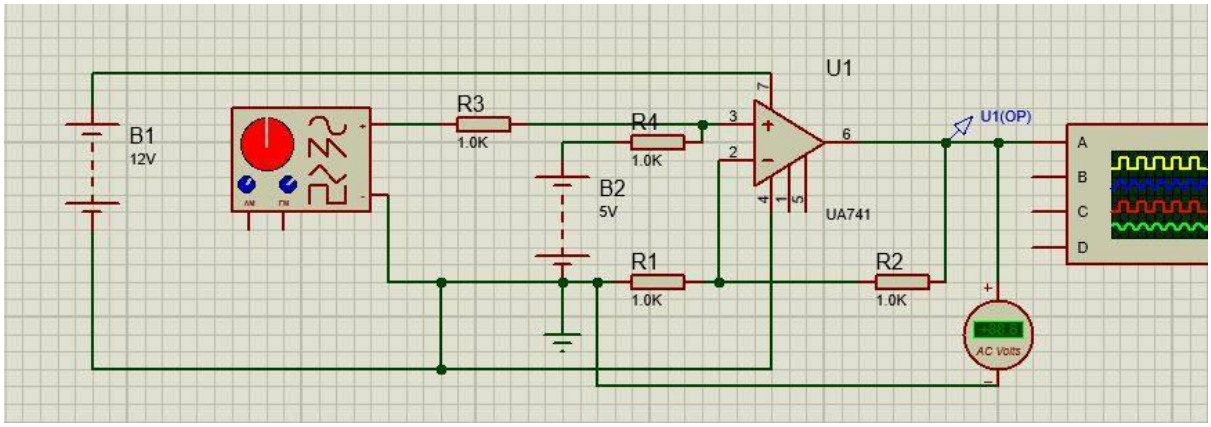

Fig 3.2: Proteus Design of Circuit B

In the second attempt, this circuit was built. In this circuit, 12V positive voltage was used instead of 5V like the previous one. In this circuit, the signal was not also in the linear region. It was tried to add an offset to take the signal to the linear region of the amplifier but this attempt also didn't go well as the IF signal was distorted by the offset.

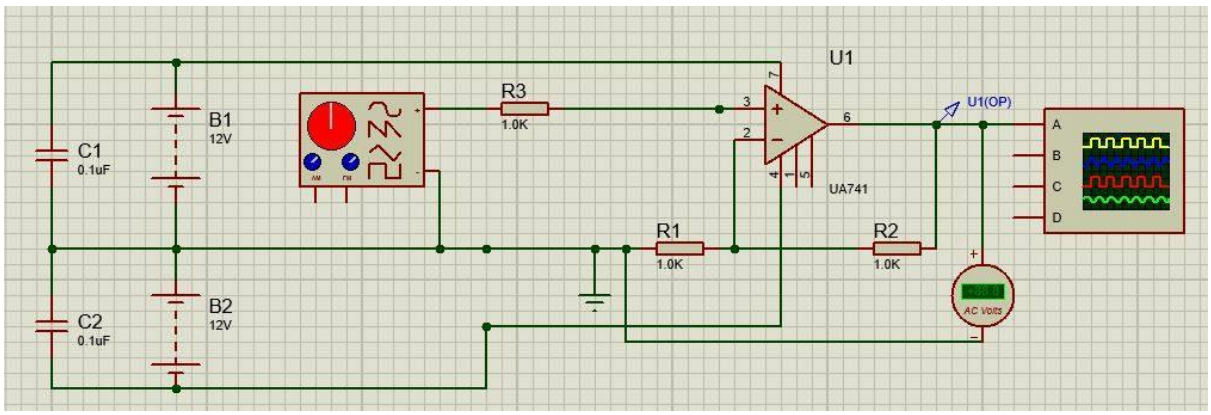

Fig 3.3: Proteus design of Circuit C

In this design, at first dual power was used to provide negative voltage at the Vin of the amplifier. By this way, the problem of linear region was overcome. But still there was problem regarding the noise in the output signal because the used Op AMP wasn't robust in noise cancelling.

Primary Design Evaluation:

Proposed Final Design-

Upon evaluating our previous attempt, we used INA811p instrumentation amplifier for amplifying the IF signal. We fabricated the amplifier using dual power supply (using 2 Li-Po batteries). Also we recommended 20 times amplification for better data acquisition by ADC. The amplification range was fixed using a potentiometer. 2 capacitors were connected between the power supply and ground for cancelling out power line interference.

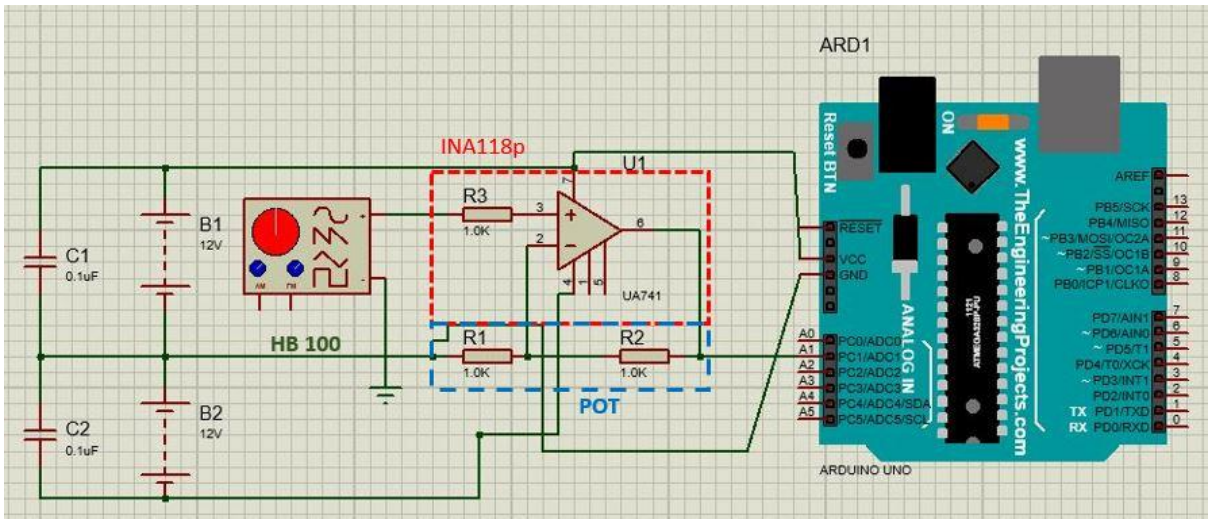

Fig 4.1: Proteus design of final amplifier circuit

The output of the amplifier was then connected to Arduino Nano for ADC, framing and serial communication. The Arduino was programmed using Arduino IDE. For serial communication from Arduino to PC, Both serial port (COM) and Bluetooth device were used. For Bluetooth connection TX and RX of the module were connected to the RX and TX of the Arduino. We further noticed a cascaded square wave in the Power line (5V) due to the Bluetooth module which added additional noise in data acquisition. So the Bluetooth module was isolated powered by another Arduino module. The overall system was powered by 2 batteries.

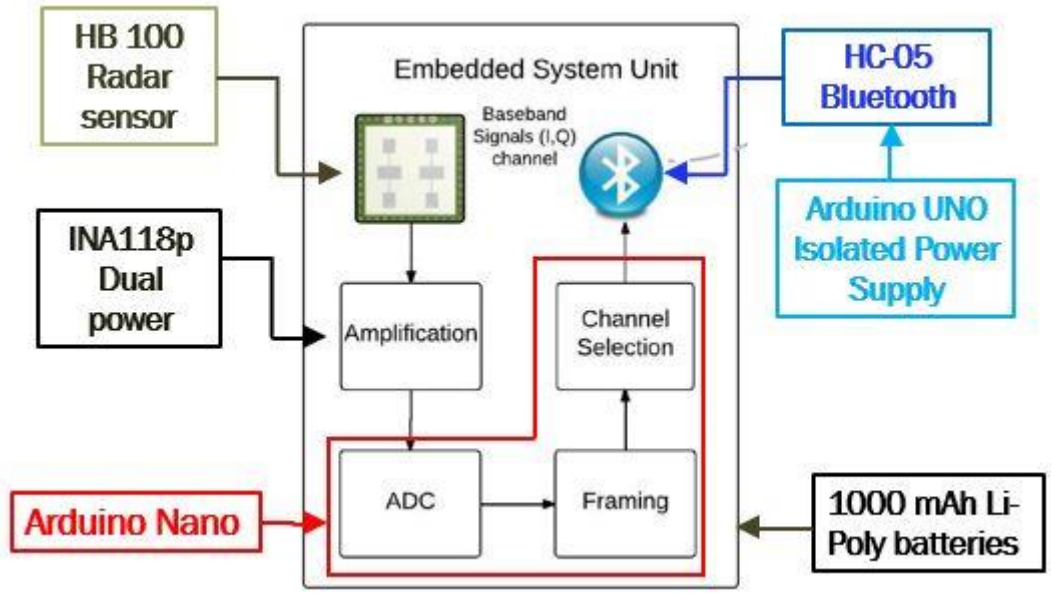

Fig 4.2: Schematic of proposed final design.

Fabrication Process

Materials-

There were several factors of research works when building the prototype. At first, the selection of Doppler radar sensor. Doppler radar sensor is not available in Bangladesh. So, we got 2 Doppler radar sensor from USA. CDM 324 and HB 100.

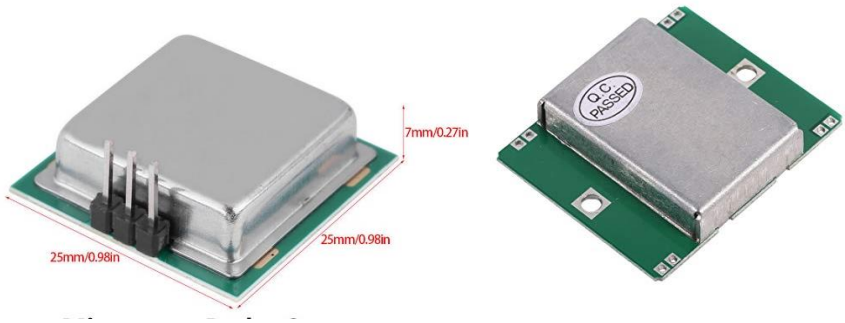

Figure 5.1: CDM 324 and HB 100 Doppler Radar sensors from left to right

After some trial and error and literature review, HB 100 was chosen to work with. For signal acquisition, several amplifier circuit was designed. After doing several trial Amplifier INA 118P was chosen.

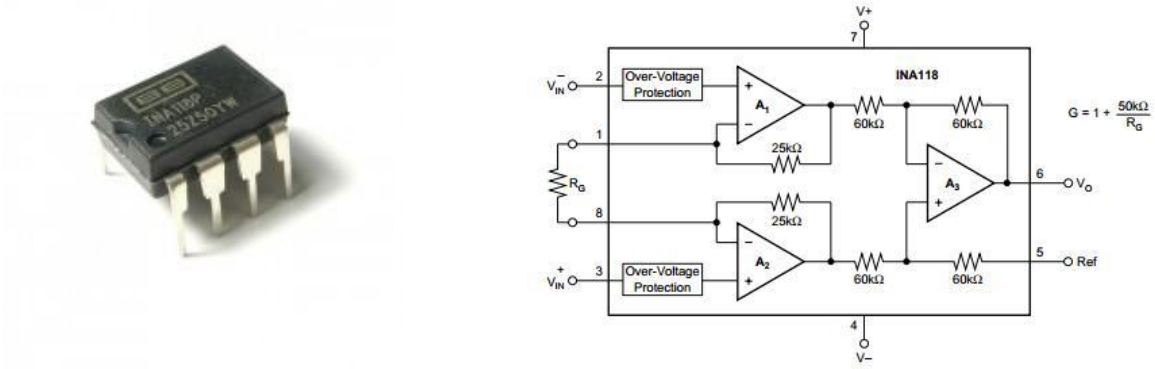

Figure 5.2: Amplifier Module INA 118P and circuit diagram

For acquisition of signals, Arduino and Bluetooth module was used. Arduino Uno and Arduino Nano both are used in the final prototype. HC-05 Bluetooth module served the purpose.

Figure 5.3.1: Bluetooth HC-05

Figure-5.3.2: Arduino Uno

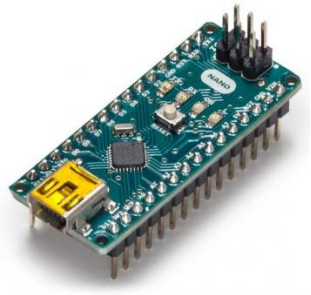

Figure 5.3.3: Arduino Nano

Finally for powering up the circuit, 12V Li-Po batteries were used.

Figure 5.3.4: 12 V Li-Po Battery

Methods-

Hardware:

1. All the components were connected according to the Proteus circuit design.
2. The circuit was fabricated on both the breadboard and the Vero board to evaluate the performance.

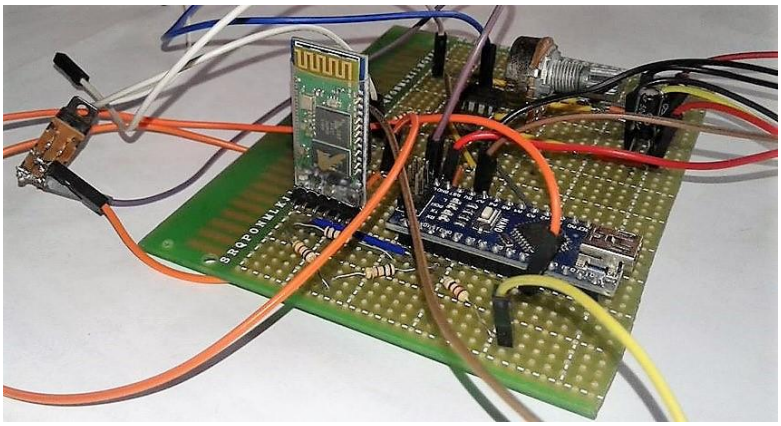

Fig: Circuit fabricated on Vero board

3. Arduino, Bluetooth and Radar sensor were powered up by 2 Li-Po batteries. One of them was for positive e and other was for negative power supply.
4. A 3D printed casing was designed using SolidWorks design software and printed using PLA which is a convenient 3D printing materials. The whole

circuit were later confined in a designed 3D printed cage. All the design are in the appendix.

Fig: 3D printed case

Software:

1. Data were transferred from Arduino through Serial Communication or Bluetooth device (TX, RX).
2. The transmitted data were received and processed by Matlab software.
3. For serial communication the data was accessed using COM serial port and Data acquisition toolbox and scanned the data using Matlab functions in real time. For Bluetooth communication, Bluetooth SPP using Instrument control toolbox in Matlab.

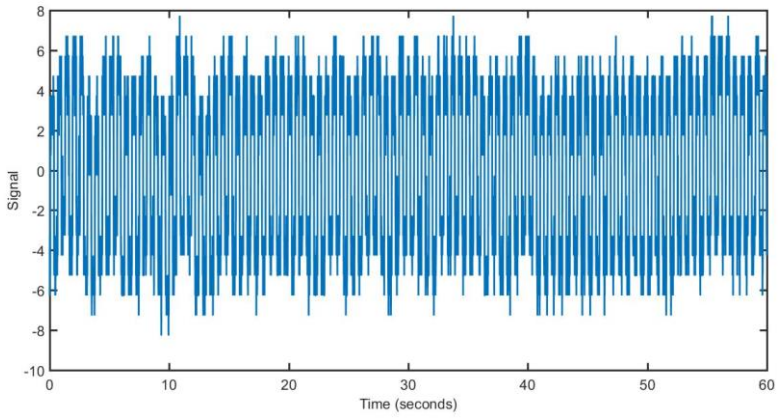

Fig 7.1: **Raw Data collected in MATLAB with 100 Hz sampling frequency and 60s durations.**

4. Data processing Algorithm was developed and applied on the collected dataset which is described in the following part.
5. Normal human breathing range is about 12 to 18 breaths per minute. So the IF signal which contains the breathing part should be within 0.3 to 0.5 Hz frequency range. To evaluate the hypothesis we used the raw data and did a power density spectrum using Fast Fourier Transform (FFT). From the single sided Fourier transform we observed that about 80% of the signal power resided within 3Hz frequency of the sample, which support our hypothesis.

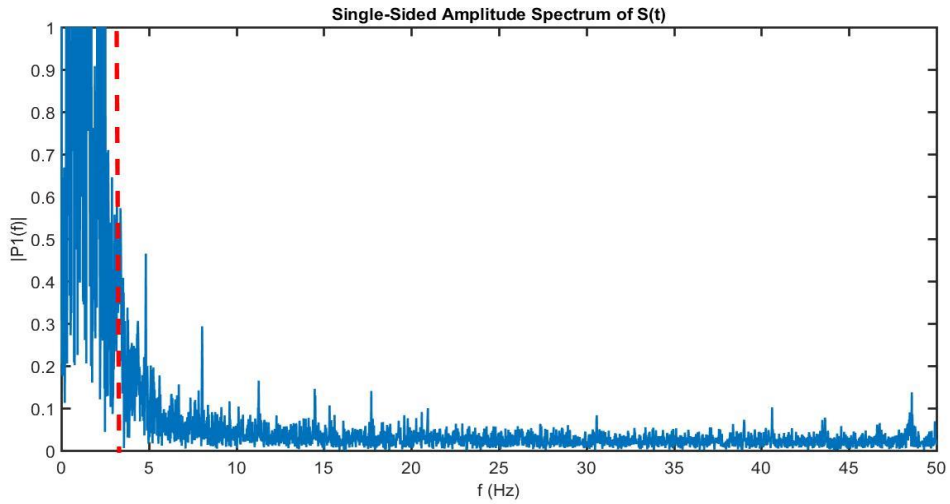

Fig 7.2: **Power Density Spectrum using FFT**

6. Later we developed a 3rd order low pass Butterworth filter with cutoff frequency at 0.3 Hz and filtered the raw data. Butterworth filter is widely used in biomedical signal processing. Furthermore we smoothed the data using 35 sample moving average filter.

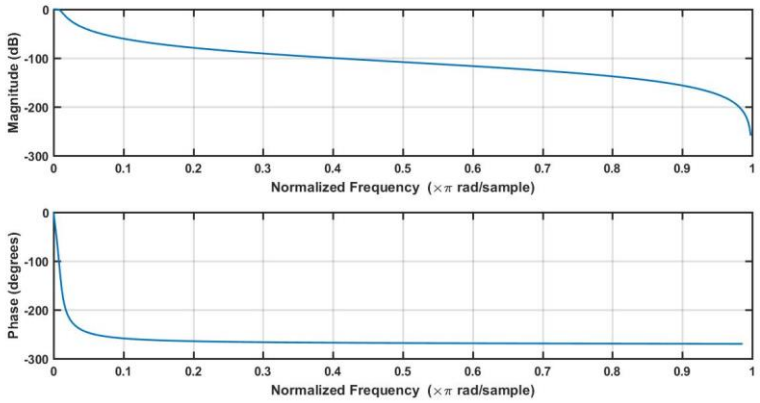

Fig: Magnitude and phase response of the Butterworth filter.

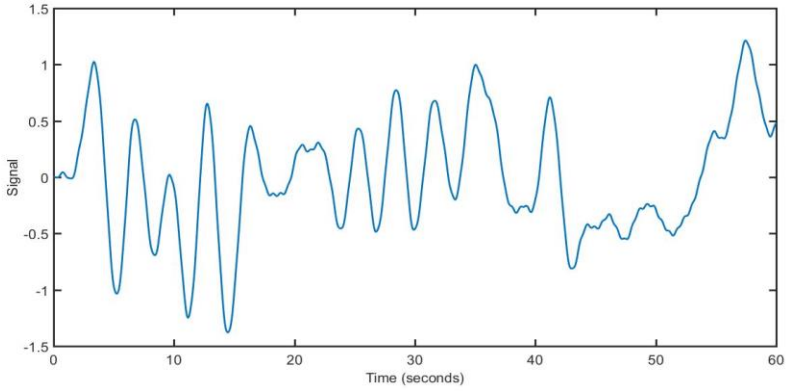

Fig 7.3: **Filtered Data**

7. In order to locate each breathing in the signal, we used cross correlation method and correlated the signal with a known breathing pattern. The known pattern was calculated using the signal power and estimated breathing pattern frequency.

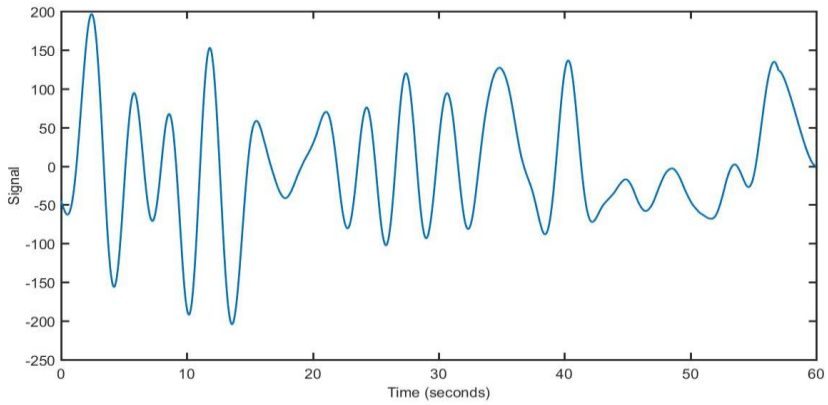

Fig 7.4: **Correlated Data**

8. Each correlated data peak represented a single breathing. Later Soothing, DE trending, and Amplitude modification were done to calculate the breathing. Here from the figure we could relate the breathing and non-breathing part within a minute. Each pick represents a single breath.

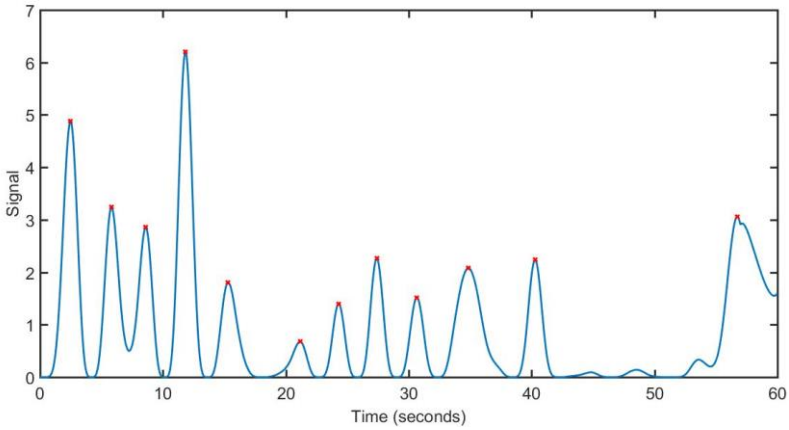

Fig 7.5: **Final Data**

9. Results were compared with reference respiration monitoring belt. 10 different sets of data were collected using respiration monitoring belt and Doppler radar sensor simultaneously for design comparison.

10. The respiration belt data was collected using LabQuest signal acquisition hardware and displayed on the LoggerPro software.
11. The Doppler radar data was processed using the Matlab algorithm. The comparison of both data set were discussed in the later part.

Final Prototypes

Hardware:

The finalized hardware was encapsulate in the fabricated 3D case. For fabrication we used the breadboard version of the design.

(a)

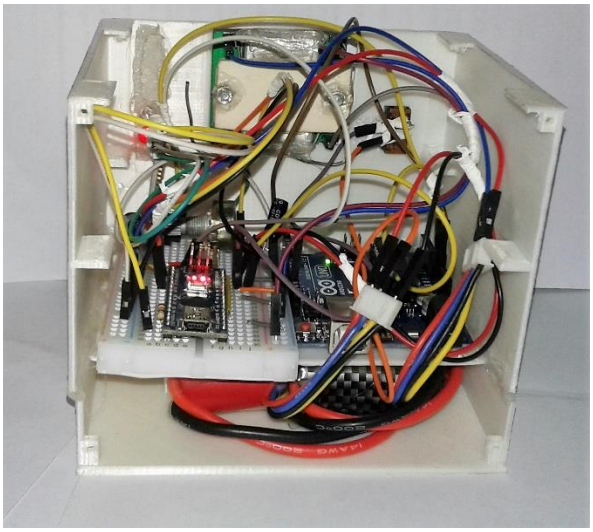

(b)

Fig 6.1: Final Circuit Design for Hardware

Here the lower compartment of the case contained the batteries, middle section contained the Arduino and the circuit and the upper section contained the Doppler radar sensor. A switch and LED were fabricated for operating purpose.

Software:

For better data visualization, a Matlab based GUI was developed using 'Matlab App Designer'. By entering the time duration for data collection, the breathing pattern can be visualized at approximate 15 s delayed time.

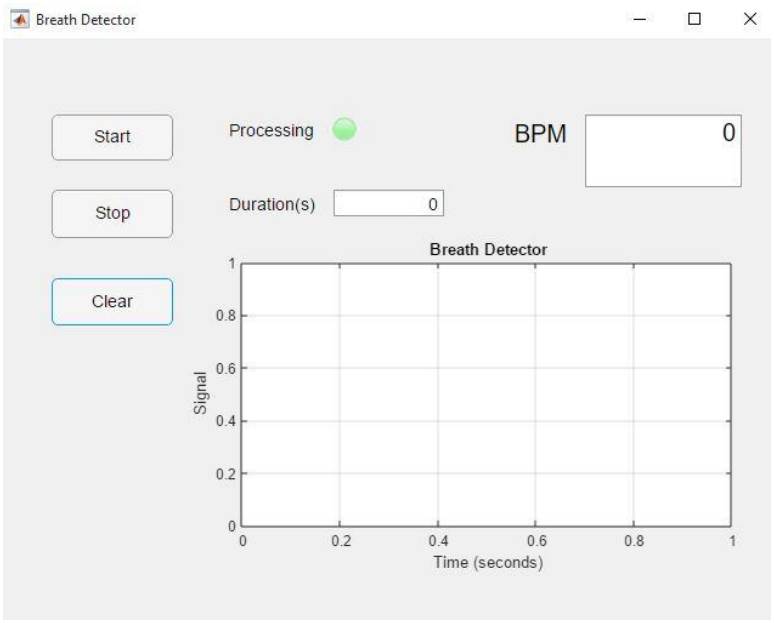

Fig: Matlab GUI for breathing pattern visualization.

Data Collection and Testing

1. For evaluation purpose, 2 different types of data set were collected using both the respiration belt and Doppler radar sensor.
2. The first type was continuous breathing while sitting in a chair. Both the data set contained breathing pattern with environmental noise.

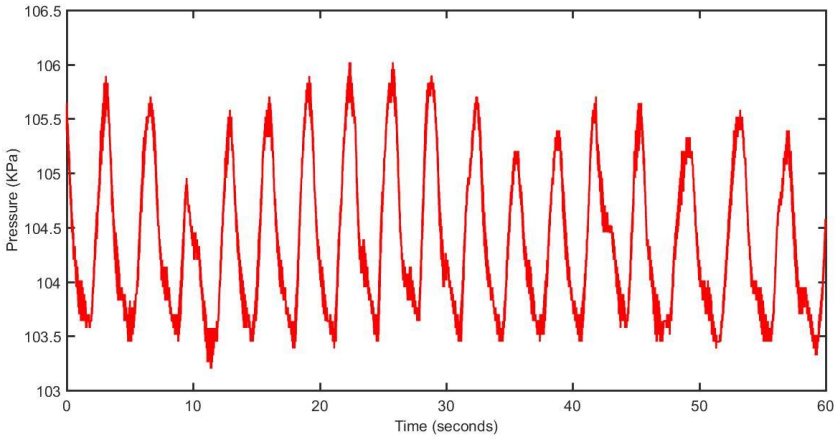

Fig: Respiration belt data collected from Logger pro for first type. The data was sampled at 100Hz and the duration was 60s.

The Doppler radar was processed using the algorithm for comparison.

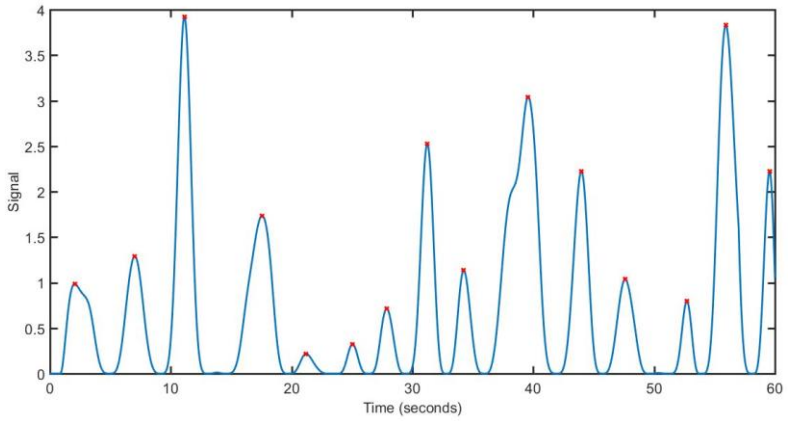

Fig: Breathing pattern using the Doppler radar.

3. In second type the data was collected for no breathing condition. Both the respiration belt and Doppler radar dataset contained only environmental noise and body movement data.

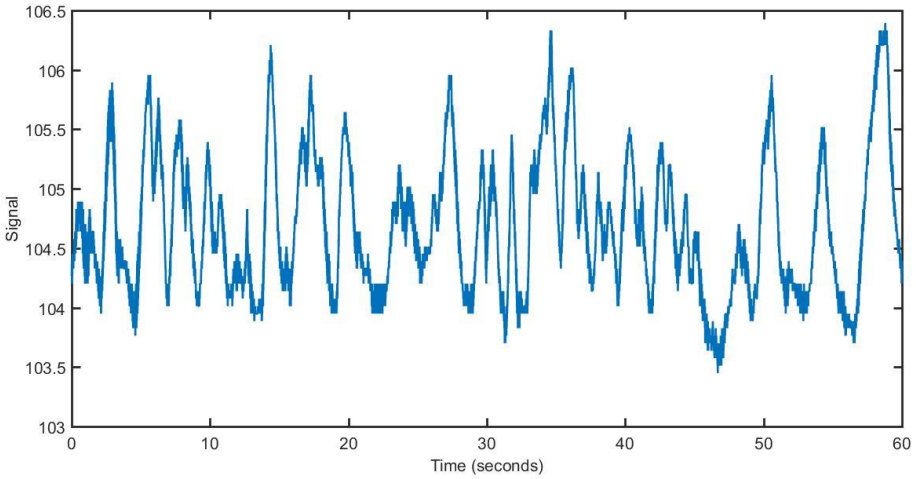

Fig: Respiration belt data collected from Logger pro for second type (containing environmental noise, body movement). The data was sampled at 100Hz and the duration was 60s.

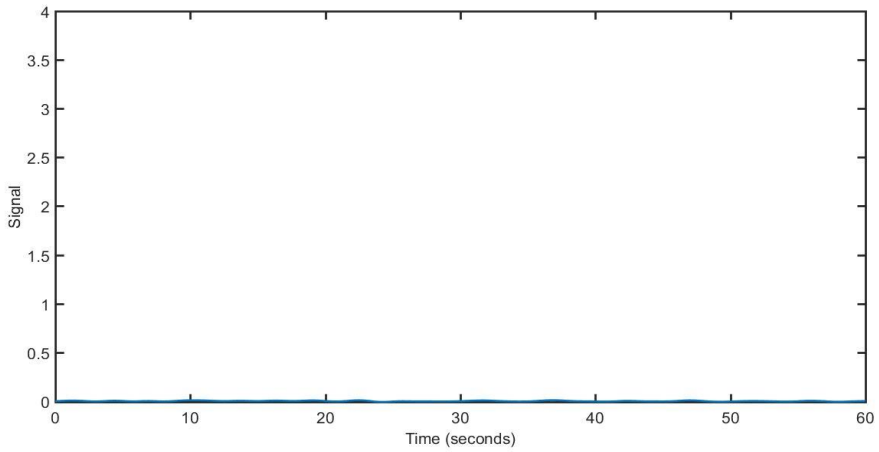

Fig: Doppler radar data. The algorithm perfectly cancel out any environmental noise.

Result

For first type of breathing data, the breathing rate calculated from the respiration rate was 17 Breaths per minute (BPM). But the breathing rate calculated from Doppler radar sensor was 15 BPM. Here the error occurred due to system data loss while transmission and acquisition as 15 s data frame was collected at a time and due to the code run time. But the success rate was almost 88%.

For second type of breathing data, only the environmental noise was present in the data set. The respiration belt data showed large fluctuation of pressure and breathing pattern like signal output. As for the Doppler radar data, after processing through algorithm, no breathing pattern were shown. From this observation, it is clear that the algorithm can cancel out noise successfully and it is robust.

Discussion:

In this report, the design, implementation, and evaluation of a contactless unobtrusive respiration monitoring system is described. The validation of the feasibility of this monitor in a lab setting and in the wild was done and results show that this monitor can detect breathing rate with an error rate of 8.07%. Based on this results, by combining vital signal estimation with movement tracking, this monitor can show great promise for continuous, passive, unobtrusive sleep monitoring.

Doppler radar sensor is extremely sensible to different types of noises. By learning about its working principles, it is known that any types of movement is detected by the Radar sensor. As a result, physical movements, environmental noises and any other sources of noises are detected at the output signal. In this project, our main challenge was to make the breathing pattern visible after filtering and smoothing it out from all of the noises. The algorithm and the filter that we have designed works well with all of the previously mentioned conditions but still there can be some errors. The cut off frequency of the filter was kept at 0.3 Hz. So, a noise of 0.3 Hz will not be filtered and can come at the output as a source of errors.

The whole circuit is connected with wires. So, there can be some problem in connections of wires which can be a potential source of errors. Bluetooth device always

introduce an offset in the signal as well as during Bluetooth transfer of data, noise can be introduced and some errors can occur.

The processing of the signal like filtering, smoothing etc. are done in MATLAB. So, during the transfer of dataset, some time lag still exists and the capacity to transfer data of Bluetooth module is also limited. As a result, a lag always exists in real time visualization of the breathing pattern and breathing rate.

Conclusion:

In a nutshell, present respiration monitoring systems cannot address some special medical condition well like in the case aged, burnt and neonatal conditions. A contactless continuous monitoring system can come to help in this regard. In this project, it is aimed to come to a solution to address that specific medical conditions.

This project designates an efficient investigation about the performance of Doppler Radar sensor for unobtrusive continuous respiration monitoring. The performance of the monitor was compared with reference respiration monitoring belt and appreciable results were also found. Wireless characteristics of the sensor and portability has made the project significant. By this project, it can be said in certain that special application based respirators can be efficiently designed through Doppler Radar sensor with availability, portability, accuracy and cost effectiveness.

The methodology of signal processing algorithm which is presented here can be modified, intensified and implemented for more accuracy and more sophisticated performance. Several work can be done for the aesthetics and commercial availability of the product. Additionally, for future works, the method should be associated with sleeping stage monitoring and to diagnose sleeping disorder conditions. Working on more better and efficient algorithm can be the foremost priority in future. More work can be done on real time visualization and development of mobile application to make the use of the device more accessible to common people.

References:

Adatya, S., Bennett, M. K., Anand, J., Singh, S. K., Antoun, D. G., Cohn, W. E., … Hochman, J. S. (2014). Percutaneous Mechanical Support in Cardiogenic Shock: A Review. *Annals of Cardiothoracic Surgery*, *3*(6), 179–187. https://doi.org/10.3978/j.issn.2225-319X.2014.08.24

Balossino, R., Gervaso, F., Migliavacca, F., & Dubini, G. (2008). Effects of different stent designs on local hemodynamics in stented arteries. *Journal of Biomechanics*, *41*(5), 1053–1061. https://doi.org/10.1016/j.jbiomech.2007.12.005

Berry, J. L., Santamarina, A., Moore, J. E., Roychowdhury, S., & Routh, W. D. (2000). Experimental and computational flow evaluation of coronary stents. *Annals of Biomedical Engineering*, *28*(4), 386–398. https://doi.org/10.1114/1.276

Dubé, H., Clifford, A. G., Barry, C. M., Schwarten, D. E., & Schwartz, L. B. (2007). Comparison of the vascular responses to balloon-expandable stenting in the coronary and peripheral circulations: Long-term results in an animal model using the TriMaxx stent. *Journal of Vascular Surgery*, *45*(4), 821–827. https://doi.org/10.1016/j.jvs.2006.12.012

Gould, K. L. (1991). Coronary Artery Stenosis, 323. https://doi.org/10.1308/003588406X106432

Hara, H., Nakamura, M., Palmaz, J. C., & Schwartz, R. S. (2006). Role of stent design and coatings on restenosis and thrombosis. *Advanced Drug Delivery Reviews*, *58*(3), 377–386. https://doi.org/10.1016/j.addr.2006.01.022

Hsiao, H.-M., Lee, K.-H., Liao, Y.-C., & Cheng, Y.-C. (2012). Cardiovascular stent design and wall shear stress distribution in coronary stented arteries. *Micro & Nano Letters*, *7*(5), 430. https://doi.org/10.1049/mnl.2011.0590

Jenei, C., Balogh, E., Szabó, G. T., Dézsi, C. A., & Kőszegi, Z. (2016). Wall shear stress in the development of in-stent restenosis revisited. A critical review of clinical data on shear stress after intracoronary stent implantation. *Cardiology Journal*, *23*(4), 365–373. https://doi.org/10.5603/CJ.a2016.0047

Kastrati, A., Mehilli, J., Dirschinger, J., Pache, J., Ulm, K., Schühlen, H., … Schömig, A. (2001). Restenosis after coronary placement of various stent types. *American Journal of Cardiology*, *87*(1), 34–39. https://doi.org/10.1016/S0002-9149(00)01268-6

Kiran, U., & Makhija, N. (2009). Patient with Recent Coronary Artery Stent Requiring Major Non Cardiac Surgery. *Indian Journal of Anaesthesia*, *53*(5), 582–591.

Ku, D. N., Giddens, D. P., Zarins, C. K., & Glagov, S. (1985). Pulsatile flow and atherosclerosis in the human carotid bifurcation. Positive correlation between plaque location and low oscillating shear stress. *Arteriosclerosis, Thrombosis, and Vascular Biology*, *5*(3), 293–302. https://doi.org/10.1161/01.ATV.5.3.293

Ladisa, J. F., Olson, L. E., Guler, I., Hettrick, D. A., Kersten, J. R., Warltier, D. C., … Pagel,

P. S. (2005). stress evaluated with time-dependent 3D computational fluid dynamics models, *53226*, 947–957. https://doi.org/10.1152/japplphysiol.00872.2004.

LaDisa, J. F., Olson, L. E., Guler, I., Hettrick, D. a, Audi, S. H., Kersten, J. R., … Pagel, P. S. (2004). Stent design properties and deployment ratio influence indexes of wall shear stress: a three-dimensional computational fluid dynamics investigation within a normal artery. *Journal of Applied Physiology (Bethesda, Md. : 1985)*, *97*(1), 424–430; discussion 416. https://doi.org/10.1152/japplphysiol.01329.2003

Lagerqvist, B., James, S. K., Stenestrand, U., Lindback, J., Nilsson, T., Wallentin, L., & the, S. S. G. (2007). Long-Term Outcomes with Drug-Eluting Stents versus Bare-Metal Stents in Sweden. *The New England Journal of Medicine*, *356*(10), NEJMoa067722. https://doi.org/10.1056/NEJMoa067722

M.A. Salehi* and A.Oladzadeh. (2013). Three-dimensional Simulation of Blood Flow in Stented Vessels and the Comparison of Wall Shear Stress in Various Stent Plans Using CFD. *JNAS Journal*, 2-S3/1076-1084. Retrieved from http://jnasci.org/wp-content/uploads/2013/12/1076-1084.pdf

Mejia, J., Mongrain, R., & Bertrand, O. F. (2011). Accurate Prediction of Wall Shear Stress in a Stented Artery: Newtonian Versus Non-Newtonian Models. *Journal of Biomechanical Engineering*, *133*(7), 074501. https://doi.org/10.1115/1.4004408

Mejia, J., Ruzzeh, B., Mongrain, R., Leask, R., & Bertrand, O. F. (2009). Evaluation of the effect of stent strut profile on shear stress distribution using statistical moments. *BioMedical Engineering Online*, *8*, 1–10. https://doi.org/10.1186/1475-925X-8-8

Scarborough, P., Bhatnagar, P., Wickramasinghe, K., Smolina, K., & Mitchell, C. (2010). Coronary heart disease statistics 2010 edition. *British Heart Foundation*, 21. https://doi.org/10.1002/hep.24445

Stents | National Heart, Lung, and Blood Institute (NHLBI). (n.d.). Retrieved July 24, 2018, from https://www.nhlbi.nih.gov/health-topics/stents

Töpel, I., Zorger, N., & Steinbauer, M. (2016). Inflammatory diseases of the aorta. *Gefässchirurgie*, *21*(S2), 80–86. https://doi.org/10.1007/s00772-016-0143-9

Types of Vascular Disease. (n.d.). Retrieved July 24, 2018, from https://www.webmd.com/heart-disease/vascular-disease#1

Rogers, C., and Edelman, E. R., 1995. \Endovascular stent design dictates experimental restenosis and thrombosis". Circulation, 91,pp. 2995-3001

(“Types of Vascular Disease,” n.d.)(“Stents | National Heart, Lung, and Blood Institute (NHLBI),” n.d.)

Appendix

LIST OF ACRONYMS

IF = Intermediate Frequency

BPM = Breath Per Minute

SPP = Serial Peripheral Interface

FFT = Fast Fourier Transform

PLA = Poly Lactic Acid

User Defined Code:

1. Arduino Code:

```
int sensorValue = 0; unsigned long T;
void setup() {
while (!Serial) {
  ; // wait for serial port to connect. Needed for native USB
}
Serial.begin(9600); }
void loop() {
sensorValue = analogRead(A3);
T=millis();
Serial.println(sensorValue);
delay(10);
}
```

2. Power spectrum density:

```
Y = fft(pressure1);
P2 = abs(Y/length(pressure1));
P1 = P2(1:length(pressure1)/2+1);
P1(2:end-1) = 2*P1(2:end-1);
f = 100*(0:(length(pressure1)/2))/length(pressure1);
plot(f,P1)
title('Single-Sided Amplitude Spectrum of S(t)')
ylim([0 1]);
```

```
xlabel('f (Hz)')
ylabel('|P1(f)|')
```

3. Main Algorithm:

```
if ~isempty(instrfind)
        fclose(instrfind);
        delete(instrfind);
    end
    %%Variables (Edit yourself)
    SerialPort='COM25'; %serial port
    MaxDeviation = -100;%Maximum Allowable Change from one value to next
    TimeInterval=0.01;%time interval between each input.
    app.loop=val;%count values
    %%Set up the serial port object
    s = serial(SerialPort); %Bluetooth('HC-05',1);
    fopen(s);
    app.voltage = 0; segment_len=6000;segment_advance=1500;
    seg=1;pt=1;app.count = 2;
    y=zeros(1,segment_len); %segment is 6000 datapoint long
    %signal processing
    Fs = 100;Tsamp = 1/Fs;
    x1=y(1:end);x1=x1-mean(x1);
    t = (0:length(x1)-1)*Tsamp;
    while ~isequal(app.count,app.loop)
      app.voltage(1)=750;
      %[A,~] = fscanf(s,'%d',1);
      app.voltage(app.count) = fscanf(s,'%f'); %A
      app.voltage(1)=app.voltage(2);
      if app.count==pt+segment_advance
        ln=length(app.voltage(pt:app.count));
        ave=mean(app.voltage(pt:app.count));
        app.voltage(pt:app.count)=app.voltage(pt:app.count)-ave;
        y(4501:6001)=app.voltage(pt:app.count);
        for i=1:segment_advance+1
          if y(i)<MaxDeviation
            y(i)=y(i+1);
          end
        end
        x1=y(1:end);x1=x1-mean(x1);
        [b,a1] = butter(3,0.3/50,'low');
        y2=filter(b,a1,x1);
        t3=t(t>=0);y3=y2(t>=0);y3=y3-mean(y3);
        hoursPerDay = 35;
        coeff24hMA = ones(1, hoursPerDay)/hoursPerDay;
        y4= filter(coeff24hMA, 1, y3);
        n=1:length(y4);
        N=(max(y4)-mean(y4)).*sin((2*3.1416*0.75/300).*n);
        Z=zeros(1,length(y4));Z(1:301)=1;
        N=N.*Z;
        [acor,lag] = xcorr(y4,N);
        acor2=acor(lag>=0);
```

```
            [~, envLow] = envelope(acor2,300,'peak');
            acor3=acor2-envLow;acor3(acor3<0)=0;
            acor3=acor3/rms(acor3);acor3=((acor3).^2)./2;
            acor3(acor3<0.5)=0;acor3=acor3.*10;
            acor3(acor3<=mean(acor3)/4)=acor3(acor3<=mean(acor3)/4)./10;
acor3(acor3>=mean(acor3)*2)=(acor3(acor3>=mean(acor3)*2)./20)+mean(acor3)*2;
            for in=fliplr(length(acor3)-500:length(acor3))
              if acor3(in)>mean(acor3)/4 && acor3(in)>acor3(in-1)
                acor3(in)=0;
              else
                break;
              end
            end
            acor3=smooth(acor3);
            plot(app.UIAxes,t3,acor3);hold(app.UIAxes,'on');
            kpre=1;index=0;
            for k=2:length(acor3)-1
              if (acor3(k)>acor3(k-1)&& acor3(k)>acor3(k+1)&& acor3(k)>mean(acor3)/2 &&
abs(t3(k)-t3(kpre))>=1)
                plot(app.UIAxes,t3(k),acor3(k),'rx');
                index=index+1;kpre=k;
              end
            end
            hold(app.UIAxes,'off');
            BPM=(index*4)/seg;
            app.BPMTextArea.Value=num2str(BPM);
            if seg>4
              seg=4;
            else
              seg=seg+1;
            end
            y(1:4501)=y(1501:6001);
            pt=app.count;
          end
          pause(TimeInterval);
          app.count = app.count +1;
        end
        for i=1:length(app.voltage)
          if app.voltage(i)<MaxDeviation
            app.voltage(i)=app.voltage(i+1);
          end
        end
        assignin('base','value',app.voltage);
        app.ProcessingLamp.Enable='off';
        fclose(s);
        delete(s);
        clear s;
```

CAD Design:

Solidworks design of the casing:

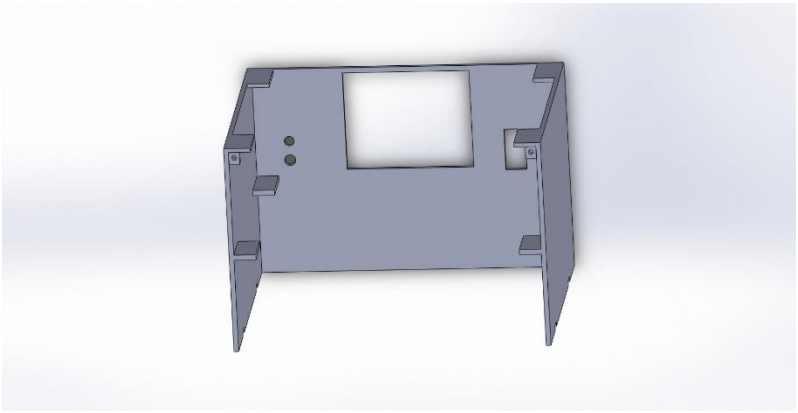

Fig: Front cover.

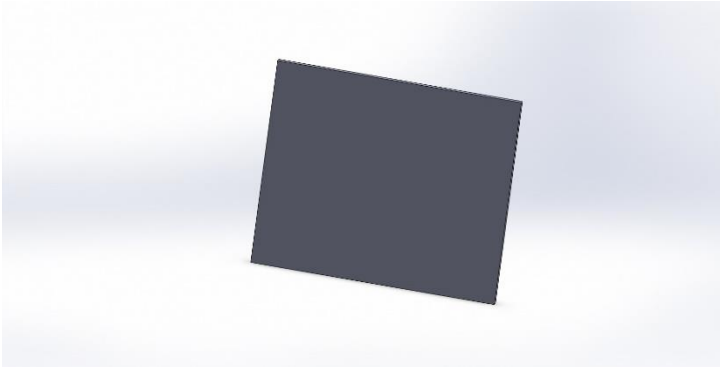

Fig: Upper cover.

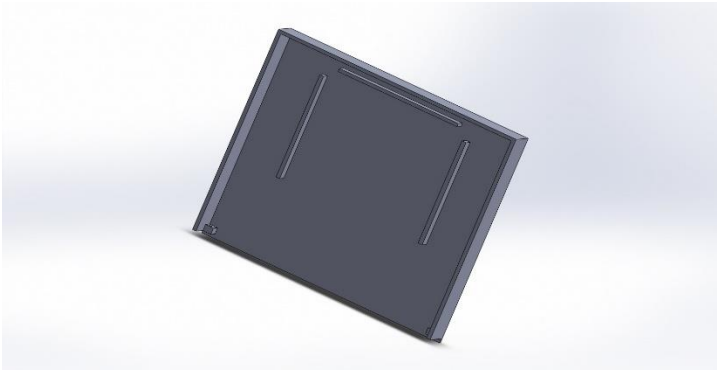

Fig: Basement.

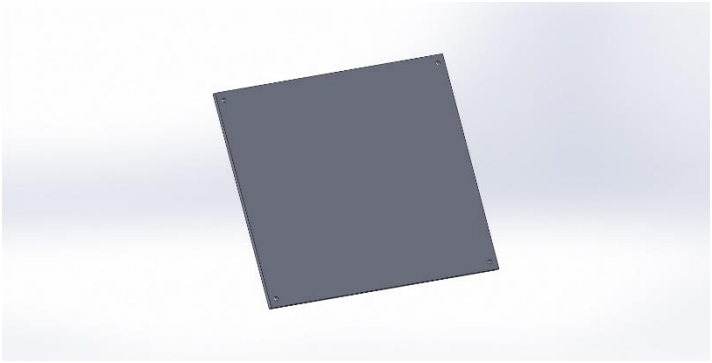

Fig: Back cover.

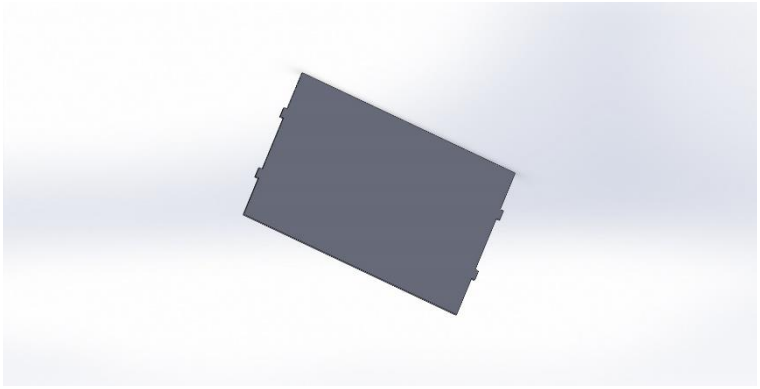

Fig: Circuit holder.

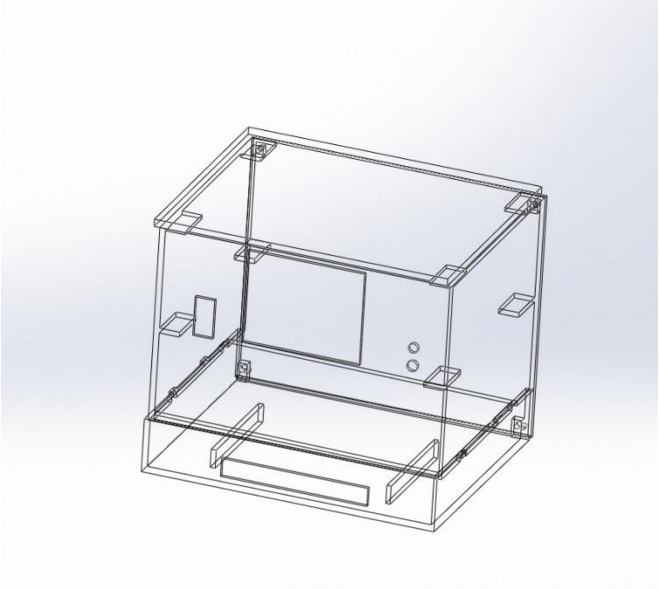

Fig: Arranged view of the casing.